JOURNAL OF MATERIALS SCIENCE 30 (1995) 4125–4132

Corrosion resistance of composite TiN–TiC layers deposited on tool steels by different techniques

E. LUNARSKA
Institute of Physical Chemistry, Polish Academy of Sciences, 01-224 Warsaw, ul. Kasprzaka 44, Poland

J. MICHALSKI
Institute of Precision Mechanics, Warsaw, Poland

TiC layers were formed by the low-pressure chemical vapour deposition (LPCVD) technique on tool carbon steel (0.9 wt % C; 0.4 wt % Si; 0.5 wt % Mn), bare or nitrided by glow discharge with formation of zones consisting of $(\varepsilon + \gamma')$ and (γ') phases. The composite TiN–TiC layers were formed by the deposition of TiN on the coated TiC layers, by a pressure-assisted chemical vapour deposition (PACVD) technique or by TiC sputtering in nitrogen under glow discharge conditions. The electrochemical behaviour of the metal/coating has been established by potentiodynamic tests done in acid (20% H_3PO_4) and alkaline (0.1 N NaOH) solutions. The deposited layers protect the steel by decreasing the steel area exposed to the aggressive solution and by promoting steel passivation. The protective ability of composite TiN/TiC layers is higher than that of corresponding single layers. Improvement of the protective ability of LPCVD TiC layers is achieved by the deposition conditions, providing the formation of fine grains $\langle 1\,1\,1 \rangle$ texture. The electrochemical behaviour of steel coated with complex TiN/TiC layers approaches the intrinsic electrochemical behaviour of TiN.

1. Introduction

One of the main targets for TiN or TiC deposition on steel is the improvement of corrosion resistance. The protective effect of coatings depends on their chemical composition [1–3], thickness [2, 3], microstructure [2, 4–6], as well as on their cohesion to the substrate material, which is in turn affected by the composition and properties of the auxiliary layers underneath the exposed surface [1, 4]. The formation of laminate structure, thus would provide the best solution for achieving the optimum combination of corrosion and wear resistance.

The aim of this work was to evaluate the corrosion and electrochemical behaviour of steel coated with composite TiN–TiC-nitrided layers deposited by different techniques in order to establish the effect of film morphology and structure on corrosion protection of steel.

2. Experimental procedure

Samples (20 mm diameter and 4 mm thick of carbon tool steel (0.9 wt % C; 0.4 wt % Si; 0.5 wt % Mn) were used as the substrate. The parameters of the deposition processes are shown in Table I. TiC layers were deposited on bare or pre-nitrided substrate by the low-pressure chemical vapour deposition (LPCVD) method using a $TiCl_4$–H_2 mixture. The nitriding of steel with the formation of a surface zone containing $(\varepsilon + \gamma')$ compounds and the (γ') diffusion zone was produced by glow discharge in a $H_2 + N_2$ atmosphere. Some of the samples coated with TiC were over-covered with TiN by pressure-assisted chemical vapour deposition (PACVD) or by sputtering titanium carbide by nitrogen under glow discharge conditions.

The facilities for producing layers by the LPCVD and PACVD methods have been described earlier [7, 8].

The phase composition of the coatings was identified by X-ray diffraction (XRD) using CoK_α radiation; the prevailing texture was estimated by comparison of relative intensity [9]. Optical microscopic examination of coatings at magnifications up to $\times 1000$ was done on the sample cross-section after etching with Murakami reagent. SEM examination of the specimen surface topography was carried out before and after corrosion tests.

The resistance of the coated materials to environmental action was established in electrochemical tests. The specially designed electrochemical microcell was placed on the sample surface covering an area of 0.045 cm^2 and the same specimen (total surface about 3.0 cm^2) can be tested under different conditions.

20 % H_3PO_4 (pH 1) and 0.1N NaOH (pH 12) were used as the acid and alkaline electrolytes, respectively. Phosphoric acid was chosen because in that electrolyte, carbon steel exhibits active dissolution and

0022–2461

TABLE I Parameters of the deposition processes

Sample code	Coatings	Coating methods	Atmosphere	P (hpa)	H_2 ($dm^3 h^{-1}$)	N_2 ($dm^3 h^{-1}$)	$TiCl_4$ ($g h^{-1}$)	t (h)	T (K)
C1	TiC/steel	LPCVD	$TiCl_4$–H_2	10	22	–	10	4.5	1123
C2		LPCVD						4.5	1173
C3		LPCVD						4.5	1273
CN	TiC/nitrided steel	LPCVD	$TiCl_4$–H_2	10	22	–	10	4.5	1273
NC1	TiN/TiC	TiN sputtering	N_2	3	–	3	–	1	1023
		TiC by LPCVD	$TiCl_4$–H_2	10	22	–	10	4.5	1123
NC2	TiN/TiC	TiN by PACVD	$TiCl_4$–H_2–N_2	3	3	3	5	1	993
		TiN by LPCVD	$TiCl_4$–H_2	10	22	–	10	4.5	1173
N	TiN/steel	TiN by PACVD	$TiCl_4$–H_2–N_2	3	22	3	5	1	993

passivation, depending on the applied potential [6]. The cell open circuit potential, E_c, was monitored for 0.5 h. The polarization data (current vs. potential relationship) was recorded with the shift of potential into the anodic direction, starting from the potential -800 mV up to $+1600$ mV, with a potential scan rate of 600 mV min^{-1}. All potential values are given versus the Hg/HgO electrode, which was used to avoid possible contamination of the near electrode electrolyte; ($E_{Hg/HgO} = 0$ corresponds to $+100$ mV in the hydrogen electrode scale).

The following parameters were estimated from the polarization data: corrosion current density, i_c, established as the current density on the cathodic polarization curve corresponding to the corrosion potential; the maximum anodic current density, i_a; passivation potential, E_p; passive current density, i_p. Values of i_a and E_p were established only in the case of acid solution. The passive current density was established as the minimum value of current in the passive region in acid electrolyte and as the current corresponding to 0 mV in alkaline electrolyte.

Corrosion current density is accounted for by the corrosion rate. Corrosion potential, passivation potential and passive current density describe the ability of material for passivation. The maximum anodic current density describes the intensity of the active metal dissolution; in the case of a metal covered with a layer it may also characterize the "electrochemical" porosity of the layer.

3. Results

3.1. Coatings composition

The X-ray diffraction (XRD) results for specimens coated under different conditions are shown in Fig. 1.

Estimation of the layer's texture shows that at 1123 K the TiC crystals (C1) grow along the (1 1 1) preferred orientation which corresponds to the growing direction ⟨1 1 1⟩, cf. Fig. 1a. As deposition temperature increases, the tendency of the TiC crystals to grow along the (4 0 0) preferential orientation, corresponding to the ⟨1 0 0⟩ growth direction becomes more pronounced, cf. Fig. 1a, samples C2 and C3.

The layers deposited at 1273 K on bare steel (C3) and on pre-nitrided substrate (CN) contain only the TiC phase, cf. Fig. 1a and b. Thus, during the course of TiC deposition in a $TiCl_4$–H_2 atmosphere, the nitrogen present in the substrate does not participate in the process of layer formation.

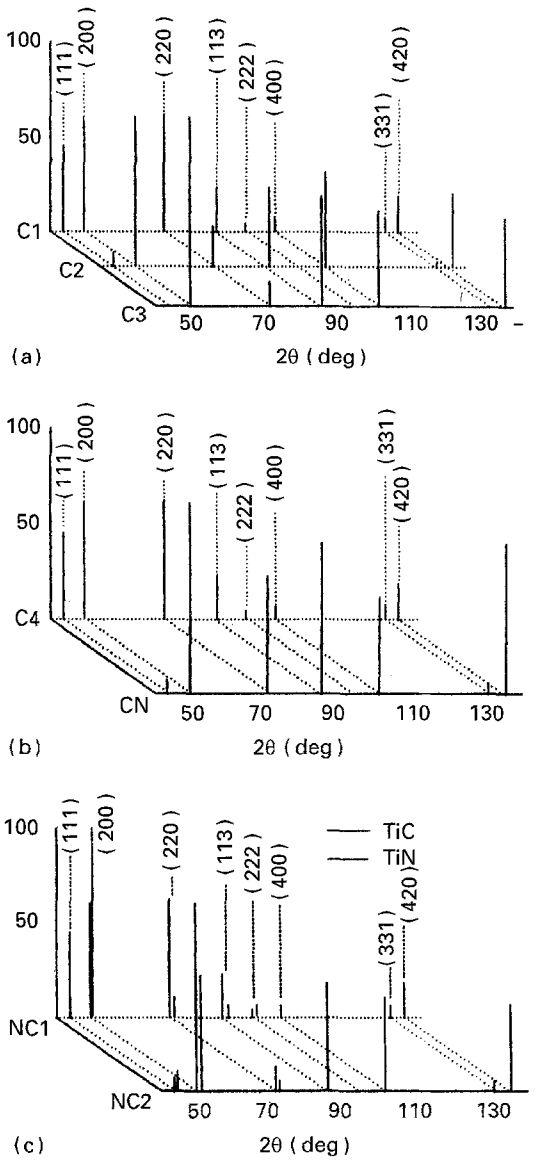

Figure 1 Schematic X-ray diffractograms of steel covered with a layer deposited under different conditions. (a) LPCVD TiC layers: C1, 1123 K; C2, 1173 K; C3, 1273 K. (b) LPCVD TiC layers deposited on bare steel substrate (C3) and on pre-nitrided substrate (CN). (c) Composite TiN/TiC layers; TiN formed by TiC sputtering by nitrogen under glow discharge conditions (sample NC1) and by PACVD technique (sample NC2). hkl values are indicated along the lines.

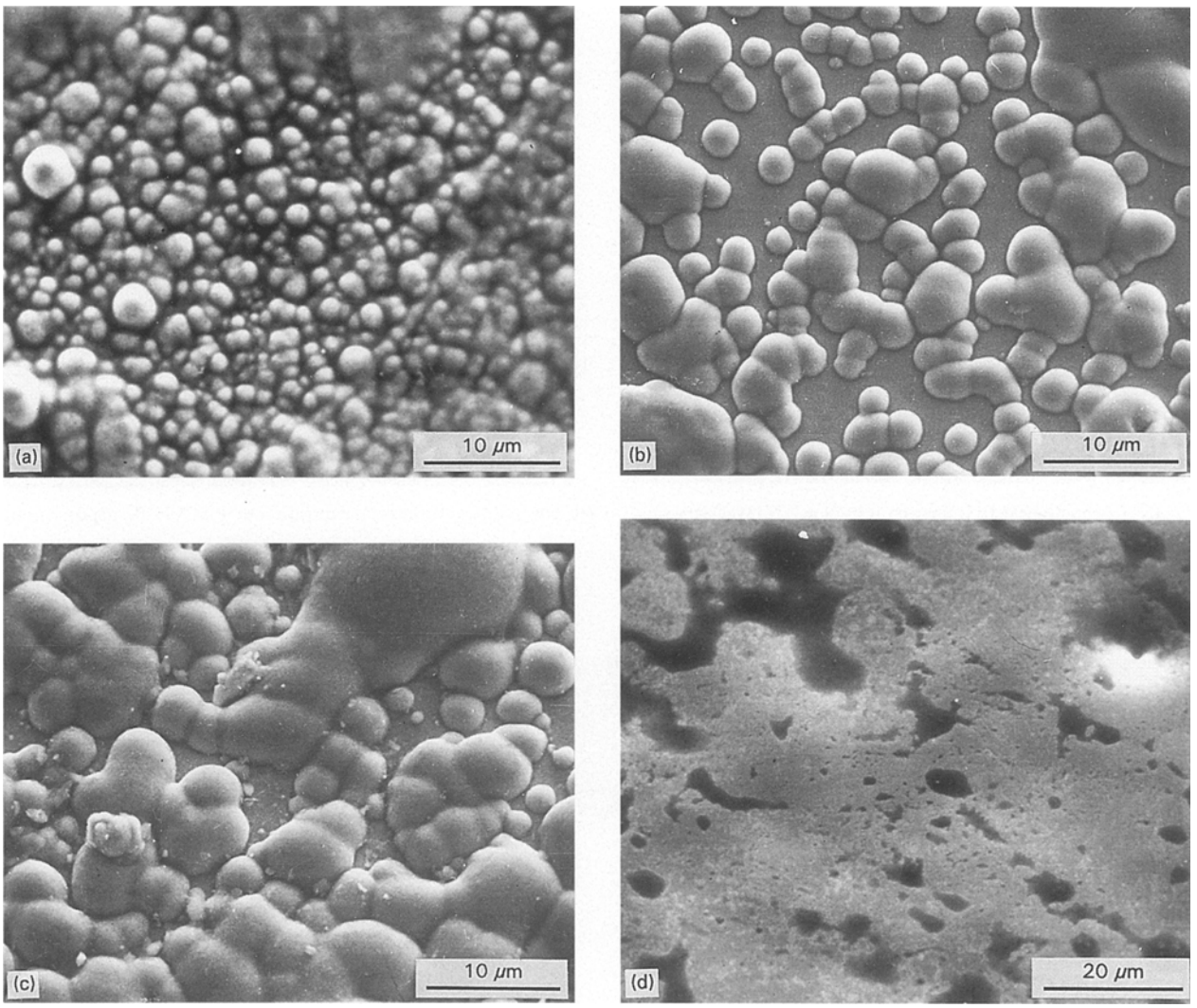

Figure 2 Scanning electron micrographs of TiC layer deposited at different temperatures: (a) 1123 K (C1); (b) 1173 K (C2); (c, d) 1273 K (C3, CN); (a, b, c) deposition on bare steel; (d) deposition on pre-nitrided steel.

Fig. 1c shows the X-ray results for the composite coatings TiN/TiC (samples NC1 and NC2). In both cases, the diffraction lines of TiC as well as those of TiN are seen. This means that in specimen NC1, the surface zone of the previously deposited TiC layer underwent transformation to TiN during the sputtering process.

3.2. Coating structure

Fig. 2 shows the topography of TiC-coated specimens. TiC deposited on bare steel is nodular and isolated at first. The size of the nodules increases with increasing temperature and nodular bridging occurs to a large extent. TiC deposition on pre-nitrided steel (Fig. 2d) results in a smooth and lustrous surface.

Topography of specimens with TiN deposited on TiC (NC1 and NC2) also reveals the nodular appearance, as seen in Fig. 3. A more diffuse bridging of the nodules is apparent in Fig. 3a. Sputtering of titanium carbide by nitrogen under glow discharge conditions (NC1 specimen) causes the development of this surface, cf. Fig. 3a and b.

Fig. 4 presents the typical microstructure of deposited layers. In all cases the layer consists of almost equiaxial grains, no columnar nor fibrous grain structure has been found. Some cracks are seen within the layers, cf. Fig. 4a. The grain size of the TiC layer formed on bare steel is larger than that formed on a pre-nitrided surface at the same temperature, cf. Fig. 4a and b. Sputtering causes the formation of a thin but quite continuous outer TiN layer, cf. Fig. 4c.

The values of thickness and grain size of the deposited layers are collected in Table II. As seen in Table II, the deposition of TiC at 1123 K (C1, NC1) causes the $\langle 1\,1\,1 \rangle$ texture, whereas at higher temperature, the $\langle 1\,0\,0 \rangle$ texture is formed.

3.3. Electrochemical behaviour

3.3.1. TiC coating

Fig. 5 presents the typical polarization curves recorded for bare steel and for C1, C2, C3 and CN specimens in H_3PO_4 solution. The characteristic electrochemical parameters are collected in Fig. 6. It is seen in Fig. 5 that polarization curves for different TiC coatings are similar to that for bare steel; an active dissolution region exists in all coatings. However, TiC coatings shift the corrosion potential into the more anodic direction and shift the passive potential into the cathodic direction (Figs 5 and 6a). Thus, the decrease in the potential range of active dissolution

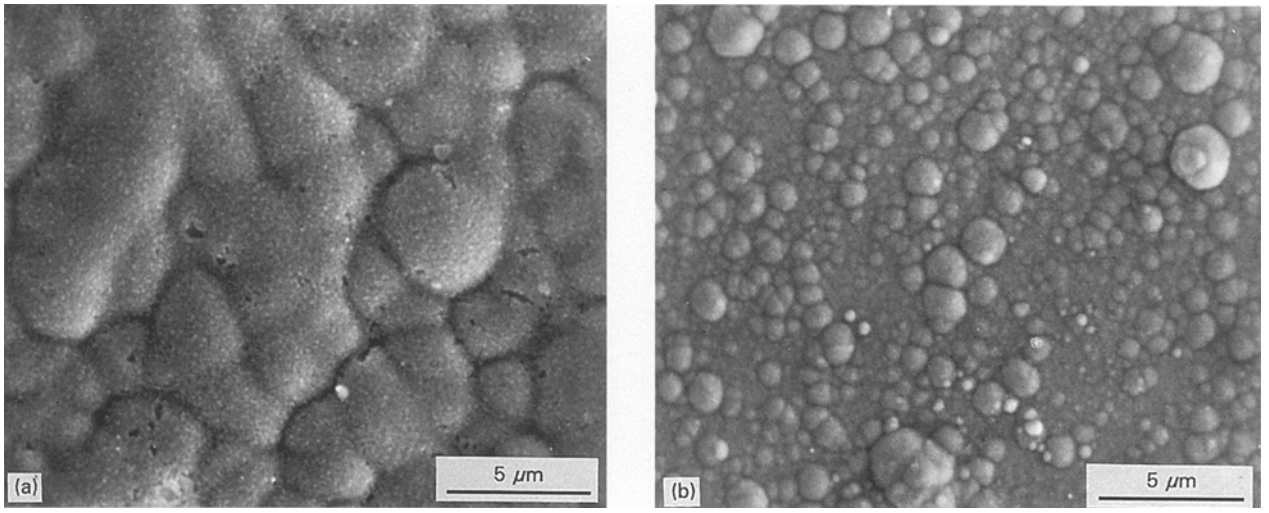

Figure 3 Scanning electron micrographs of a TiN layer deposited on TiC covered steel surface: (a) deposition by PACVD; (b) deposition by sputtering.

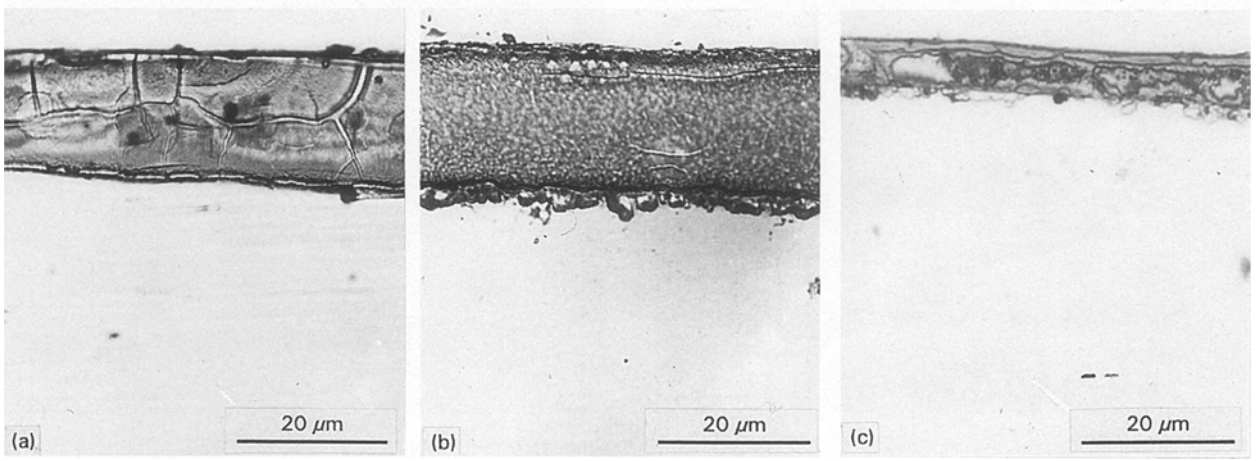

Figure 4 Microstructure of deposited layers: (a) TiC, specimen C3; (b) TiC, specimen CN; (c) TiN/TiC, specimen NC1.

TABLE II Parameters of the deposited layers

Sample code	Layer	D^a (μm)	d^a (μm)	$D:d$	Texture
C1	TiC	7	2.5	2.8	⟨111⟩
C2	TiC	12	7	1.7	⟨100⟩
C3	TiC	17	11	1.5	⟨100⟩
CN	TiC/N	22	1	22	–
NC1	TiN	1			–
	TiC	7	2.5	2.8	⟨111⟩
NC2	TiN	4	1.7	2.3	–
	TiC	12	–	–	⟨100⟩
N	TiN	4	7	1.7	–

[a] D, thickness of layer; d, mean grain size of deposits.

occurs due to coating formation in comparison with the bare steel.

TiC coatings decrease the corrosion, anodic dissolution and passive current density values in comparison with the parameters for bare steel, cf. Figs 5 and 6b. An especially pronounced effect is seen for active dissolution: anodic dissolution current density decreases more than three orders of magnitude due to the TiC formation. The values of i_α and i_c increase with increasing TiC deposition temperature, cf. Fig. 6b.

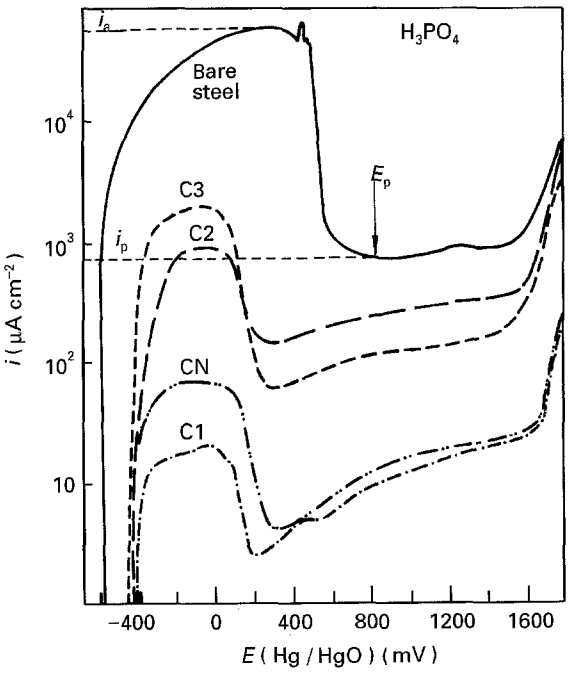

Figure 5 Polarization curves recorded in 20% H_3PO_4 (pH 1) for bare steel and for specimens covered with LPCVD TiC under different conditions. Parameters marked: i_a, anodic dissolution current density; i_p, passive current density; E_p, passive potential.

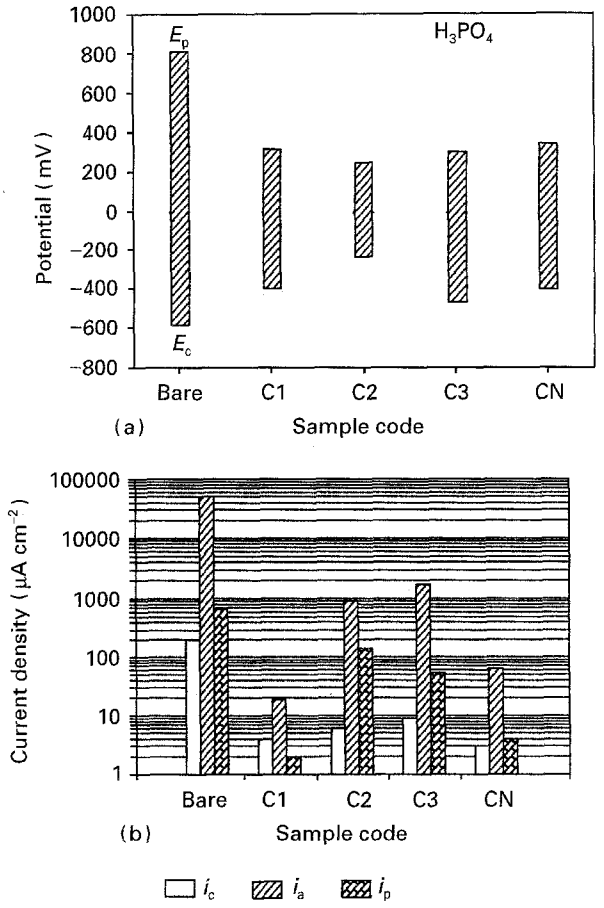

Figure 6 Electrochemical parameters for bare steel and for specimens covered with LPCVD TiC at different temperature, as tested in H_3PO_4. (a) Corrosion potential, E_c, passive potential, E_p; bars represent the active dissolution potential range. (b) Corrosion current density, i_c, active dissolution current density, i_a, passive current density, i_p.

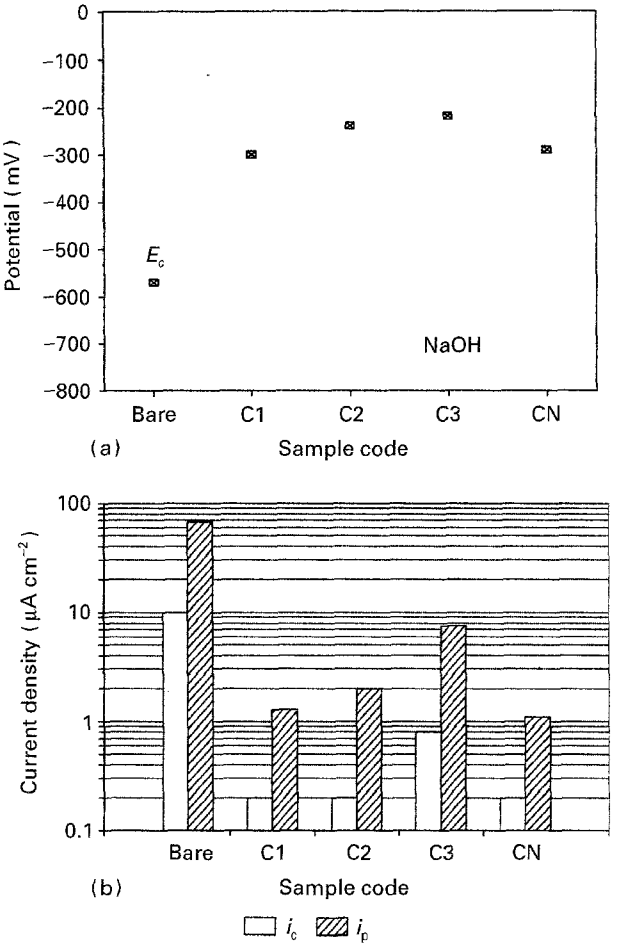

Figure 8 Electrochemical parameters estimated for bare steel and for specimens covered with LPCVD TiC under different conditions, as tested in NaOH: (a) corrosion potential, E_c, (b) corrosion current density, i_c, passive current density, i_p.

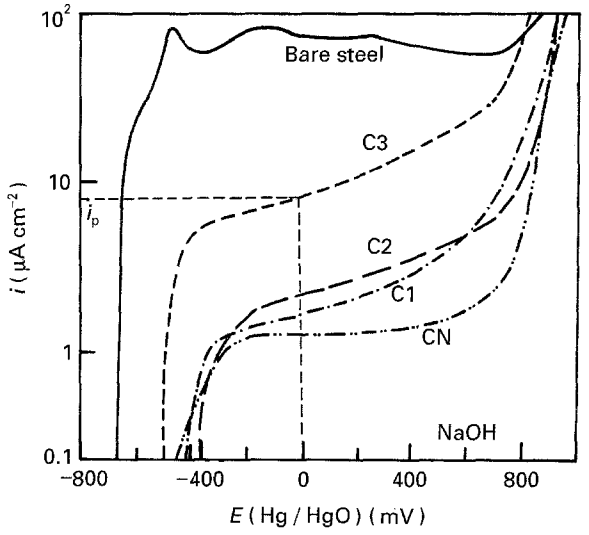

Figure 7 Polarization curves recorded in 0.1 N NaOH (pH 12) for bare steel and specimens covered with LPCVD TiC under different conditions; i_p, passive current density.

Deposition of TiC on pre-nitrided steel (specimen CN) causes a decrease in i_c, i_α and i_p values as compared to those for TiC coating deposited at the same temperature on bare steel (specimen C3), cf. Fig. 6b.

Polarization curves recorded in NaOH solution are shown for bare steel and specimens C1, C2, C3 and CN in Fig. 7; the characteristic parameters are shown in Fig. 8. Similarly as in the case of pH 1, TiC deposition shifts the corrosion potential into the anodic direction and decreases the corrosion and passive current density, as compared to the values recorded for bare steel, cf. Figs 7, 8a and b. The most pronounced effect is observed for TiC deposited on pre-nitrided steel.

3.3.2. TiN on TiC/coated steel

Figs 9–11 present the anodic polarization curves recorded for TiN superimposed on TiC layers on steel. The characteristic parameters are collected in Fig. 12 (pH 1) and Fig. 13 (pH 12).

At pH 1, the polarization curve for TiN-coated steel is similar to that of the single TiC layer (samples C2 and N in Fig. 9). However, TiN super deposited on TiC (NC2) shows a different trend with elimination of the active dissolution region and a general decrease in the i_c, i_α and i_p, cf. Figs 9 and 12. Sputtered TiN (NC1) causes the shift of the corrosion potential into the anodic direction by about 300 mV and almost eliminates the active dissolution, cf. Fig. 10. However, the estimated passive current density in that case is higher than that for the TiC covered specimen. TiN also decreases the potential range of active dissolution, as seen in Fig. 12a.

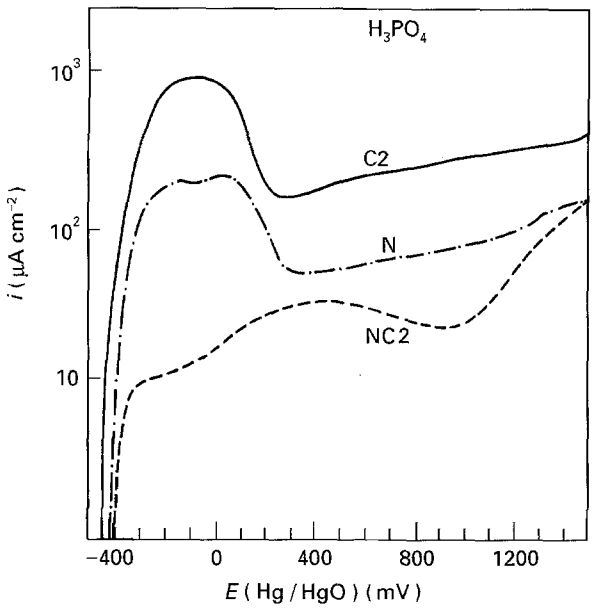

Figure 9 Polarization curves recorded in H_3PO_4 solution for specimens with a single LPCVD TiC layer (C2), a single PACVD TiN layer (N) and a PACVD TiN layer deposited on an LPCVD TiC layer (NC2).

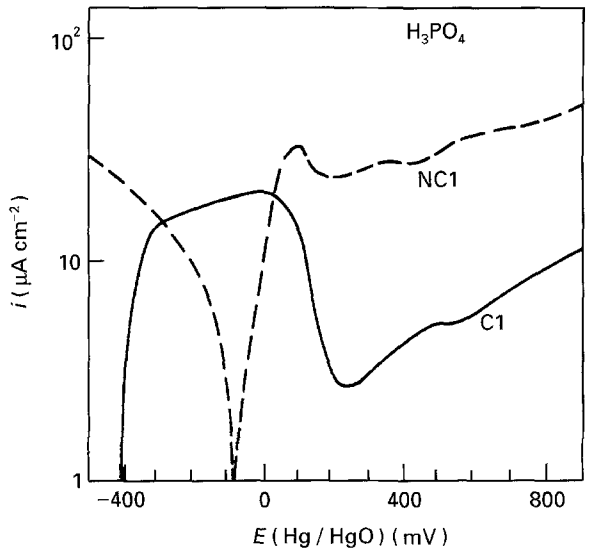

Figure 10 Polarization curves recorded in H_3PO_4 for specimens covered with a single LPCVD TiC layer (C1) and with a TiN layer deposited by sputtering of TiC by nitrogen under glow discharge conditions (NC1).

The effect of composite (TiN/TiC) layers on electrochemical behaviour at pH 12 is shown in Figs 11 and 13. Generally, the current densities (i_c and i_p) for those specimens are lower than for a single TiN layer (N) but higher than for single TiC layer (C1).

The sequences of all studied coatings according to the increase in electrochemical parameters are collected in Table III for electrolytes H_3PO_4 and NaOH. No change of surface appearance as studied by SEM has been found after the electrochemical tests.

PACVD TiN deposited on Al_2O_3 exhibited the following electrochemical parameters: $E_c = +70$ mV, $i_c = 0.12\ \mu A\ cm^{-2}$, $i_p = 1\ \mu A\ cm^{-2}$ at pH 1 and 12, $E_c = -30$ mV, $i_c = 0.1\ \mu A\ cm^{-2}$, $i_p = 1.5\ \mu A\ cm^{-2}$ in an electrolyte of pH 12.

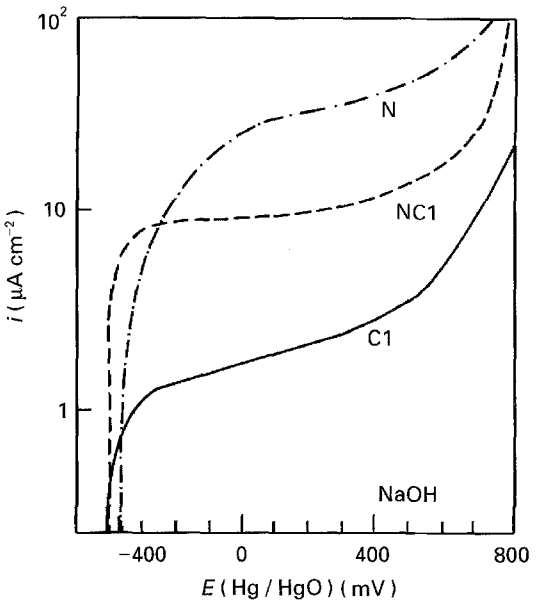

Figure 11 Polarization curves recorded in NaOH solution for specimens covered with an LPCVD TiC layer (C1), a PACVD TiN layer (N) and with a TiN layer deposited on an LPCVD TiC layer by sputtering (NC1).

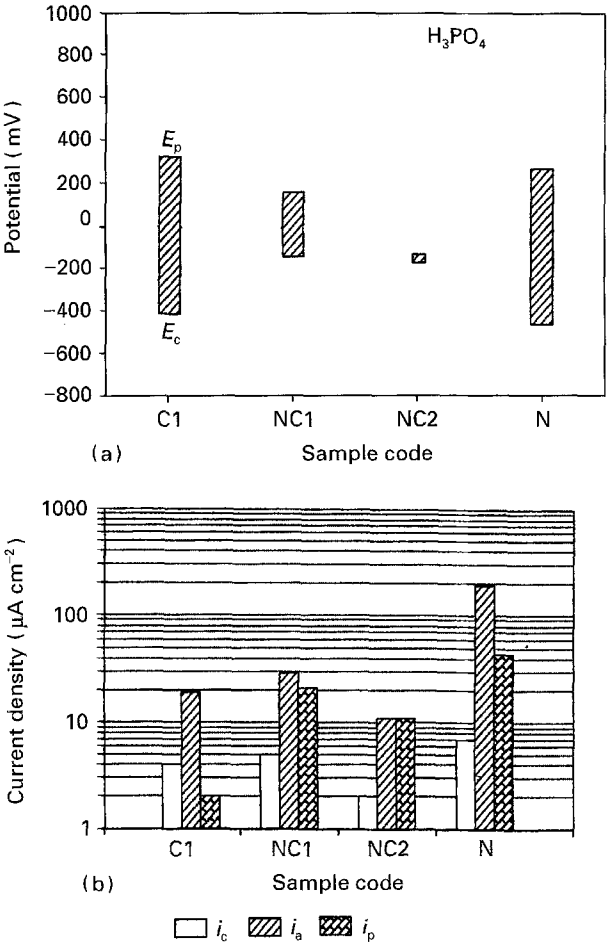

Figure 12 Electrochemical parameters estimated for steel coated with TiC (C1), TiN (N) and TiN/TiC (NC1 and NC2) as tested in H_3PO_4. (a) Corrosion potential, E_c, passive potential, E_p; bars represent the active dissolution potential range. (b) Corrosion current density, i_c, active dissolution current density, i_α, passive current density, i_p.

4. Discussion

The electrochemical behaviour of the coated metal depends on the electrochemical behaviour of the coating, on its structure and porosity, as well as on the

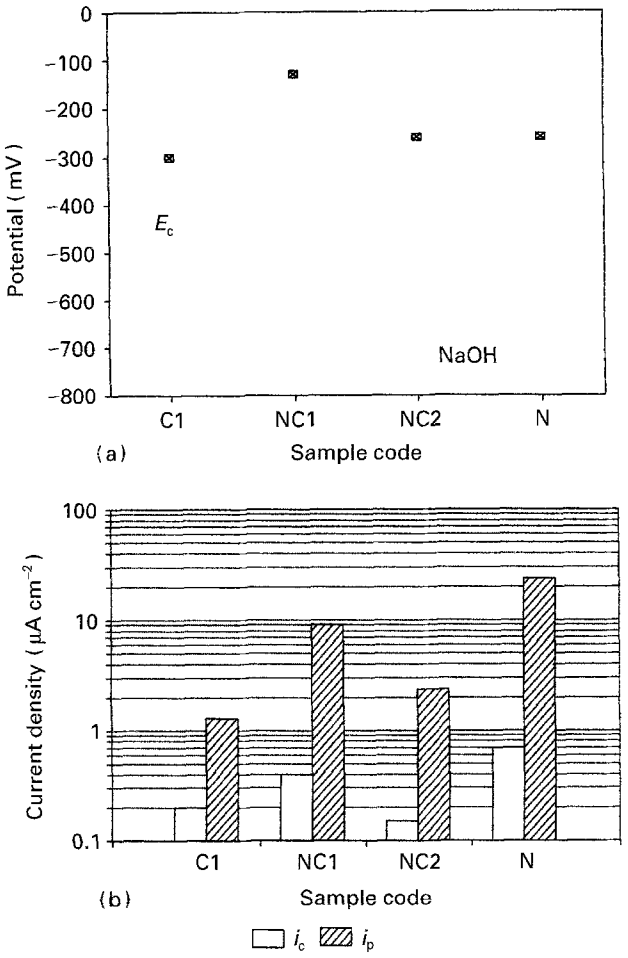

Figure 13 Electrochemical parameters estimated for steel covered with TiC (C1), TiN (N), and TiN/TiC (NC1 and NC3) as tested in NaOH. (a) Corrosion potential, E_c; (b) corrosion current density, i_c, passive current density, i_p.

TABLE III Relative effect of coatings on electrochemical parameters in H_3PO_4 and NaOH

Electrolyte	Parameter	Increasing current density
H_3PO_4	i_c	NC2 < CN < C1 < NC1 < C2 < N < C3
	i_α	NC2 < C1 < NC1 < CN < N < C2 < C3
	i_p	C1 < CN < NC2 < NC1 < N < C3 < C2
NaOH	i_c	NC2 < C1 = C2 = CN < NC1 < N < C3
	i_p	CN < C1 < C2 < NC2 < C3 < NC1 < N

electrochemical behaviour of the layer–metal interphase and substrate. The intrinsic electrochemical parameters corresponding to the coating and to the metal can be taken into account as the extreme values for the metal/coating systems. By comparing the electrochemical parameters of studied specimens in acid and alkaline solutions and relating them to the structure of the deposited layers, some tendencies could be traced.

It appears that only in the case of specimens NC1 and NC2, is the active dissolution of the substrate metal suppressed, suggesting the good coverage of the metal by TiN. In other studied cases, the deposited coatings are permeable for the electrolyte to reach the substrate and for corrosion products to leave the electrode. However, in specimens NC1 and NC2, the effect of the substrate on the electrochemical behaviour can also be seen, as follows from their comparison with the intrinsic parameters of TiN deposited on Al_2O_3 shown above. Although the i_c and i_p values for TiN/Al_2O_3 in H_3PO_4 are lower than for coated steel (Fig. 12b) the intrinsic corrosion potential of TiN (+ 70 mV) is more anodic than the corrosion potential of NC1 and NC2 specimens (Fig. 12a) revealing the effect of substrate.

The surface layer may protect the underneath metal by the decrease in surface area of metal exposed to aggressive environment or by a change in electrochemical processes.

The decrease in current density seen in Figs 7 and 9 for specimens C1, C2, C3 and CN in comparison with bare steel might be accounted for by the drastic decrease in active electrode area (steel) exposed to the solution due to the formation of an immune TiC surface layer. However, specimens covered with TiC exhibit not only a decrease in current density but also manifest a change of the characteristic potentials. A shift of corrosion potential into the anodic direction in comparison to that for bare steel shows that the TiC coating promotes the ability of the steel electrode for passivation [10]. This effect is also confirmed by shrinkage of the potential range of active dissolution in acid electrolyte in the presence of the TiC layer, cf. Figs 5 and 6. The further promotion of the surface passivation occurs at the formation of TiN/TiC composite layer.

The corrosion processes of coated metal systems must cease to a degree, as solution transport to the metal surface and the leaking out of the corrosion products are reduced or alternated, indicating that the thickness, coverage and microstructure of the coating should be involved.

Analysis of obtained data (Tables II and III, Figs 6 and 8) shows that the corrosion (electrochemical) resistivity of the studied specimens could not be accounted for by the layer thickness itself, because the specimen with the thinnest TiC coating (C1) exhibits very low corrosion, dissolution and passive current densities. The layer grain size cannot either be responsible alone for the corrosion resistivity of studied specimens. The easy paths through the layer might be associated with intergranular areas of layer. Because in all the cases the layer grains have non-columnar shape, the easy path extension may be correlated with the number of grains in the layer, i.e. with the ratio of coating thickness, D, to the grain size, d. The lower the $D:d$ ratio value, the straighter the paths from the environment to the substrate, and the relatively easier will be the transport through the layer. At high values of $D:d$ ratio, the paths become complex and transport is hindered; this inhibits the metal dissolution and promotes its passivation.

The values of $D:d$ ratio presented in Table II seem to support the above assumption. The beneficial effect of steel pre-nitriding on the corrosion resistivity can also be accounted for by the influence on TiC grain refinement. Nitriding of tool steel does not considerably improve its corrosion resistivity, but modifies the steel surface and thus promotes a more refined TiC grain nucleation.

Among the TiC-coated specimens, the highest corrosion and dissolution resistivity and the highest

ability for passivation is exhibited by specimen C1 which has the ⟨1 1 1⟩ preferential orientation and the highest number of grains within the layer thickness (the most complex paths), cf. Table II. Although the effect of paths on corrosion and dissolution discussed above could be accounted for the corrosion resistivity of C1 specimen, the effect of texture might be also taken into account. It is known [11] that the growth of small crystals is accompanied by the formation of the preferential ⟨1 1 1⟩ texture. Formation of a coarse grain layer with ⟨1 0 0⟩ texture may lead to stress relaxation by cracking of grains promoting the substrate–environment contact. Transgranular cracks have indeed been found in the case of the coarse-grained and less-corrosion resistant C2 and C3 specimens.

The other possibility is that the texture itself affects the electrochemical properties of coated metal, because the texture effect on coating hardness and wear resistance has been observed in the case of different layer orientation [12]. Although there is no information on the effect of layer texture on corrosion behaviour, it should not be neglected; the effect of texture on passivation has been established for iron single crystals [13]. Independent of the exact reason, it might be stated that the increase in $D:d$ ratio and the tendency to ⟨1 1 1⟩ texture of TiC layer decreases the susceptibility to corrosion and active dissolution of coated steel and facilitates its passivation ability.

TiN deposited by PACVD technique causes a further decrease in corrosion and passive current density in comparison with the single TiC layer.

Sputtered TiN (NC1) increases the current density in comparison with the respective single TiC layer (C1) in acid and in alkaline solutions, cf. Figs 12b and 13b. This could have been caused by the formation of TiCN having the electrochemical properties intermediate between TiC and TiN. However, X-ray (Fig. 1c) and microscopic (Fig. 4c) examinations reveal the presence of TiN as a continuous outer layer on sample NC1. Therefore, increase in current density due to TiN sputtering is assumed to be not intrinsic but an apparent effect caused by the development of the surface, as can be seen in Fig. 3a. Under the applied potentiostatic conditions, increase in the electrode surface does not change the real current density but increases the total current. Because the measured current density (i_c, i_α, i_p) is calculated for a geometrical surface of electrode, overestimating of current density occurs.

In alkaline solution, the PACVD TiN layer deposited on TiC does not distinctly improve the system's behaviour. In that solution, the passivation is already achieved by TiC deposition. Although the corrosion potential for the NC1 specimen is more anodic than for the C1 sample, the current density values are higher in the previous case. This might again be accounted for by the developing of the electrode surface as a result of sputtering. Comparing the measured corrosion and passive current density data for C1, TiN/Al_2O_3 and NC1 specimens, the assumption can be made that sputtering causes the increase in the real surface area of the specimen for several times. Taking that increase into account, the values of corrosion and active dissolution current density for the NC1 specimen in acid solution could be recalculated. Such a calculation shows that the TiN formation on the TiC layer by sputtering decreases the corrosion and dissolution, as compared with a single TiC layer.

5. Conclusions

The following conclusions concerning the effect of the deposition conditions and hence the microstructure of deposited layers on steel corrosion and electrochemical behaviour could be drawn.

1. TiC, TiN and complex layers protect steel in acid and alkaline solutions by the decrease in steel area exposed to the aggressive solution, as well as by the promotion of metal passivation.

2. The protective ability of single TiC LPCVD layers decreases with increase in the deposition temperature due to the formation of coarse grains and/or due to change in the texture from ⟨1 1 1⟩ to ⟨1 0 0⟩ orientation.

3. Formation of TiN on existing TiC layers by PACVD or by TiC sputtering by nitrogen under glow discharge conditions, dramatically improves the protective ability of the coating.

4. Composite TiN/TiC or TiC/N layers improve the protective ability of the coating in comparison with the TiN or TiC single layers.

References

1. T. ARAI, H. FUJITA and K. OGURI, *Thin Solid Films* **165** (1988) 139.
2. E. I. MELETIS, W. B. CARTER and R. F. HOCHMAN, in "Microstructural Sciences", Vol. 13, edited by S. A. Shiels, C. Bagnall, R. E. Witkowski and G. F. Vander Voort (ASM, Metals Park, OH, 1986) p. 317.
3. A. ROTHA, B. ELSNER and H. BOHNI, "Electrochemical Behavior of TiN and TiC CVD Coatings on Steels", Report, Institute for Materials Chemistry and Corrosion, Swiss Federal Institute of Technology, Zurich, ETH-Honggerberg, Switzerland (1988).
4. A. ERDEMIR, W. B. CARTER, R. F. HOCHMAN and E. I. MELETIS, *Mater. Sci. Eng.* **69** (1985) 89.
5. T. WIERZCHON, J. MICHALSKI, J. RUDNICKI, B. KULAKOWSKA and W. ZYRNICKI, *J. Mater. Sci.* **27** (1992) 771.
6. J. MICHALSKI, E. LUNARSKA, T. WIERZCHON and S. ALGHANEM, *Surf. Coat. Technol.* (1994) in press.
7. J. MICHALSKI and T. WIERZCHON, *J. Mater. Sci. Lett.* **9** (1990) 480.
8. *Idem, ibid.* **10** (1991) 506.
9. C. S. BARRET and T. B. MASSALSKI, "Structure of Metals" (Pergamon, Oxford, 1980) p. 205.
10. W. I. SHMORGUN, A. K. GORBACHEV, N. N. NECHIPORENKO, V. F. STECENKO and E. E. KRECH, *Zashchita Metallov* (*Russ.*) **14** (1978) 329.
11. J.-E. SUNDGREN, *Thin Solid Films* **128** (1985) 21.
12. J.-E. SUNDGREN and T. G. HENTZELL, *J. Vac. Sci. Technol.* **4** (1986) 2259.
13. J. KRUGER and J. P. CALVERT, *J. Electrochem. Soc.* **114** (1967) 43.

Received 14 June 1994
and accepted 3 February 1995